JOC The Journal of Organic Chemistry

Article

pubs.acs.org/joc

Joint Experimental, in Silico, and NMR Studies toward the Rational Design of Iminium-Based Organocatalyst Derived from Renewable Sources

Gabriela G. Gerosa, Rolando A. Spanevello, Alejandra G. Suárez, and Ariel M. Sarotti*

Instituto de Química Rosario (CONICET), Facultad de Ciencias Bioquímicas y Farmacéuticas, Universidad Nacional de Rosario, Suipacha 531, Rosario 2000, Argentina

Supporting Information

ABSTRACT: An efficient organocatalyst for iminium-ion based asymmetric Diels–Alder (DA) reactions has been rationally designed. The most influential structure–activity relationships were determined experimentally, while DFT calculations and NMR studies provided further mechanistic insight. This knowledge guided an in silico screening of 62 different catalysts using an ONIOM(B3LYP/6-31G*:AM1) transition-state modeling, which showed good correlation between theory and experiment. The top-scored compound was easily synthesized from levoglucosenone, a biomass-derived chiral enone, and evaluated in the DA reaction between (*E*)-cinnamaldehyde and cyclopentadiene. In line with the computational finding, excellent results (up to 97% ee) were obtained. In addition, the catalyst could be easily recovered and reused with no loss in its catalytic activity.

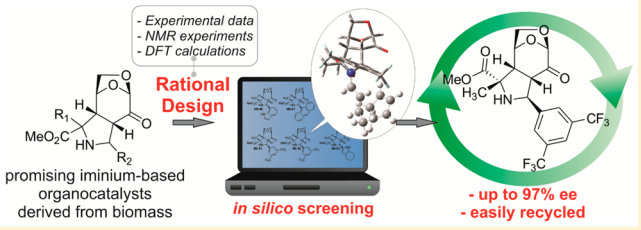

INTRODUCTION

The construction of optically active compounds continues to be of great importance in organic chemistry. In this regard, asymmetric organocatalysis has brought unprecedented progress in the last decades.[1] The use of inexpensive, metal-free, nontoxic, and often cheap organic compounds as catalysts, along with the functional group tolerance, mild reaction conditions, and high enantioselectivities in a wide scope of asymmetric reactions, represent some of the most important features.[1] These requirements are often hard to fulfill, and exhaustive experimentation by trial and error (with the concomitant investment of time, funding, and manpower) is the most common pathway toward success. Although high-throughput methods can notably speed this process, the ability to rationally design the optimal catalyst for any given transformation will probably dominate the discipline in years to come.[1h] One of the main challenges lies in anticipating how subtle structural features in the catalyst would affect the enantioselection of the system under study.

Modern computational chemistry can be particularly helpful in this area, providing a valuable insight into the mechanism, unraveling the factors influencing the stereoselectivity and facilitating the design and optimization of a wide variety of asymmetric organocatalyzed reactions.[2] Understanding the origins of the enantioselectivity experimentally found in asymmetric reactions represents the most common contribution of computational chemistry in the field.[3] In turn, this knowledge might end up guiding the design of more powerful organocatalysts. In fact, the in silico development of novel organocatalysts, rationally designed to achieve remarkable levels of stereoselection, is not uncommon.[4] However, to the best of our knowledge, the experimental verification of the computational predictions made beforehand (the ultimate goal of any theoretical model) was achieved only in few cases.[5]

Recently, we reported an efficient and straightforward synthesis of novel chiral pyrrolidines via 1,3-dipolar cycloaddition reactions between levoglucosenone (**1**), a biomass-derived chiral enone,[6] and N-metalated azomethine ylides **2** (Figure 1).[7]

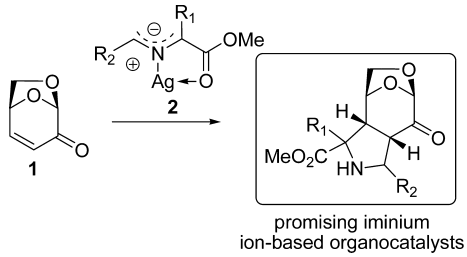

Figure 1. Chiral pyrrolidines derived from levoglucosenone as promising iminium ion based organocatalysts.

The proof-of-principle usefulness of such molecular scaffolds was demonstrated in iminium-ion based asymmetric Diels–Alder (DA) reactions between (*E*)-cinnamaldehyde and cyclopentadiene.[7] Good catalytic activity, high *exo* selectivity, and acceptable levels of enantioselection (up to 76% ee), along with the fact that the catalyst is easily derived from cheap and

Received: May 29, 2015
Published: July 15, 2015

DOI: 10.1021/acs.joc.5b01214
J. Org. Chem. 2015, 80, 7626–7634

Table 1. Effect of the Pyrrolidine Structure on the Diels–Alder Reaction between (*E*)-Cinnamaldehyde (6) and Cyclopentadiene (7)[a]

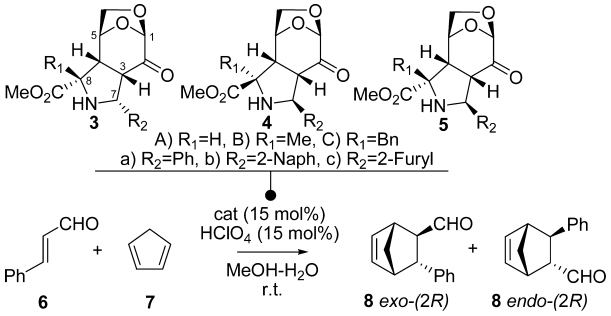

entry	cat.	R_1	R_2	time (h)	yield[b] (%)	*exo*/*endo*[c,d]	*exo* ee[d] (%)	*endo* ee[d] (%)
1				480	15	26:74		
2	**3Aa**	H	Ph	5	87	68:32	6 (2*R*)	10 (2*S*)
3	**4Aa**	H	Ph	5	97	68:32	4 (2*S*)	6 (2*R*)
4	**5Aa**	H	Ph	8	95	72:28	56 (2*R*)	54 (2*R*)
5	**3Ab**	H	2-Naph	96	71	71:29	16 (2*S*)	14 (2*S*)
6	**4Ab**	H	2-Naph	3	90	74:26	10 (2*S*)	24 (2*R*)
7	**5Ab**	H	2-Naph	5	94	76:24	44 (2*R*)	64 (2*R*)
8	**3Ac**	H	2-furyl	96	84	70:30	10 (2*S*)	0
9	**4Ac**	H	2-furyl	3	91	76:24	44 (2*S*)	10 (2*S*)
10	**5Ac**	H	2-furyl	5	96	73:27	52 (2*R*)	63 (2*R*)
11	**3Ba**	Me	Ph	20	45	68:32	4 (2*R*)	34 (2*S*)
12	**5Ba**	Me	Ph	8	98	81:19	72 (2*R*)	70 (2*R*)
13	**3Bb**	Me	2-Naph	72	66	72:28	2 (2*S*)	30 (2*S*)
14	**5Bb**	Me	2-Naph	8	99	81:19	68 (2*R*)	72 (2*R*)
15	**3Bc**	Me	2-furyl	72	42	68:32	20 (2*R*)	6 (2*R*)
16	**5Bc**	Me	2-furyl	8	97	79:21	58 (2*R*)	32 (2*R*)
17	**3Ca**	Bn	Ph	70	18	47:53	26 (2*R*)	8 (2*R*)
18	**5Ca**	Bn	Ph	48	85	82:18	80 (2*R*)	80 (2*R*)
19	**3Cb**	Bn	2-Naph	72	45	72:28	72 (2*R*)	30 (2*R*)
20	**5Cb**	Bn	2-Naph	48	87	78:22	64 (2*R*)	76 (2*R*)
21	**3Cc**	Bn	2-furyl	72	55	71:29	82 (2*R*)	52 (2*R*)
22	**5Cc**	Bn	2-furyl	48	92	80:20	84 (2*R*)	84 (2*R*)

[a]General reaction conditions: 5 equiv of cyclopentadiene, 15 mol % of catalyst, 15 mol % of $HClO_4$, MeOH/H_2O 9:1, rt. [b]Isolated yield after column chromatography. [c]Determined by ^1H NMR. [d]Determined by chiral GC.

renewable sources, encouraged us to invest efforts in the rational design of more efficient chiral organocatalysts. This article illustrates the journey to pursue our goals by means of joint experimental, NMR, and computational studies.

RESULTS AND DISCUSSION

Our initial studies were conceived to explore and understand the catalysts' structure–activity relationship in the cycloaddition between (*E*)-cinnamaldehyde (**6**) and cyclopentadiene (**7**), one of the most valuable model reactions to test the efficiency of novel iminium-based organocatalysts.[8] As shown in Table 1, the catalytic performance of 21 structurally diverse pyrrolidines **3**–**5** was evaluated using standard experimental conditions (MeOH/H_2O 9:1; 15 mol % catalyst load, 15 mol % $HClO_4$ as cocatalyst, 25 °C). This small library, which was synthesized according our previously reported procedure,[7] was chosen to introduce three dimensions of molecular diversity: the relative stereochemistry at C-7 and C-8 and the nature of the R_2 and R_1 groups at those positions, respectively. Interestingly, all of the amines under study displayed important catalytic activity compared with the thermally driven cycloaddition (entry 1), increasing up to 160-fold the reaction rate. As a general trend, the pyrrolidines with a 7(*S*) configuration (**4** and **5**) were much more reactive catalysts than the corresponding 7(*R*) adducts (**3**), clearly indicating that the relative stereochemistry of the pyrrolidinic core has a substantial influence in the reactivity of the system. On the other hand, increasing the bulkiness of R_1 (H > Me > Bn) led to longer reaction times for each series, though the aromatic moiety (R_2) at C-7 did not affect significantly the reaction rate. In contrast to the thermal cycloaddition (entry 1), all organocatalyzed reactions were *exo* selective. The levels of stereoselectivity ranged from poor to good (up to 82:18, entry 18), resulting an interesting observation considering that few organocatalysts led to a clear preference toward the *exo* isomers.[8c,d] Here again, the *exo*/*endo* ratio is largely governed by the relative stereochemistry at C-7 and C-8 of the pyrrolidine and the nature of R_1. While *endo* adducts **3** afforded the lowest levels of *exo* selectivity, its C-7 epimers (**5**) led to the most selective reactions, mainly those bearing a quaternaty center at C-8 (R_1 = Me or Bn).

Last, the asymmetric induction capacity of the evaluated amines ranged from poor to very good (up to 84% ee, entry 22). The *exo* catalysts **4**, the most reactive under study, afforded unsatisfactory levels of enantioselection (up to 44% ee, entry 9). Similar observations were made with the pyrrolidines with

DOI: 10.1021/acs.joc.5b01214
J. Org. Chem. 2015, 80, 7626–7634

endo stereochemistry (compounds **3**), which with the exceptions of two cases (entries 19 and 21), also gave poor ee's (up to 34%, entry 11). In contrast, compounds **5** afforded the highest facial selectivities (44%−84% ee for *exo* adducts; 32%−84% ee for *endo* adducts). In this case, the substitution at both C-7 and C-8 affected the reaction outcome. Regarding the nature of R_1, a general trend was observed: bulkier groups at C-8 lead to higher ee's, as the derivatives of phenylalanine (R_1 = Bn) are the most selective organocatalysts under study. On the other hand, the effect of the aromatic moiety at C-7 depends on the substituent at C-8. For instance, R_2 = Ph is preferred when R_1 = H or Me, while R_2 = 2-furyl gave better results when R_1 = Bn.

In summary, the best overall results were obtained with **5B** (R_1 = Me) and **5C** (R_1 = Bn), but considering a balance between reactivity and selectivity the former (**5B**) was identified as the most promising core for further optimization. Although **5C** afforded the highest *exo*/*endo* and enantiomeric ratios, the selectivities achieved with their analogues **5B** were slightly inferior but with a great improvement in the reactivity of the system.

Turning now to the reaction mechanism, whose knowledge is critical for rational design purposes, the proposed catalytic cycle is depicted in Scheme 1. Condensation of the catalysts **3**−**5**

Scheme 1. Proposed Catalytic Cycle

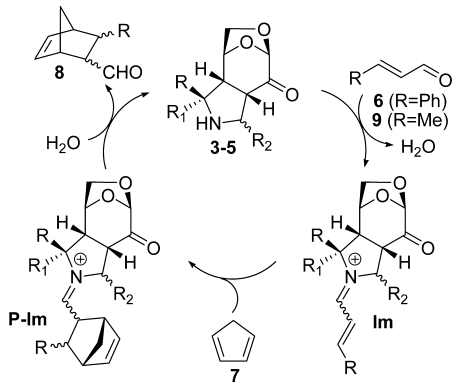

with aldehyde **6** generates the iminium intermediate **Im**. The formation of this positively charged species lowers the LUMO energy of the *α*,*β*-unsaturated moiety, leading to a more reactive dienophile. This step is crucial in the success of the catalytic system, by both increasing the rate and allowing facial discrimination in the [4 + 2] cycloaddition to cyclopentadiene. Finally, iminium adducts **P-Im** hydrolyze to release the desired adducts *endo*- and *exo*-**8** (in both enantiomeric forms) and regenerate the catalyst for the next cycle.[9]

To gain more evidence and provide confidence in theoretical models for further optimization, we undertook a B3LYP/6-31G* computational study of the reaction between (*E*)-crotonaldehyde (**9**) and cyclopentadiene, both thermally driven and catalyzed by compound **5Ba**. Figure 2 shows the most stable conformations found for the isomeric (*E*) and (*Z*) iminium ions derived from the condensation of **5Ba** and **9**.[10] Our calculations suggest that the (*Z*) isomer is 2.47 kcal/mol less stable than the (*E*) isomer, due to steric repulsion between Ha/C-7 and Hα/CH_3 in the former.

Conceptual DFT analysis provided a theoretical explanation for the notable acceleration of the catalyzed reactions.[11] The global electrophilicity index (*ω*), which measures the

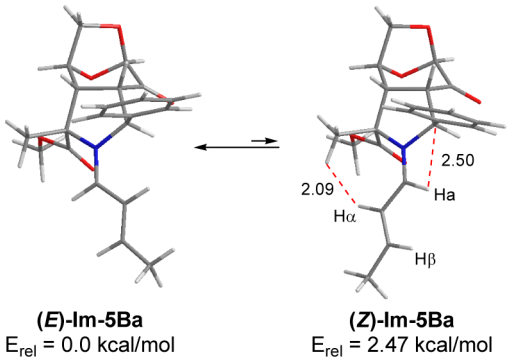

Figure 2. B3LYP/6-31G*-optimized geometries found for (*E*)- and (*Z*)-iminium ion derived from the condensation between **5Ba** and **9**.

stabilization energy when the system acquires an additional electronic charge Δ*N* from the environment,[12] is much higher for (***E***)**-Im-5Ba** than that for (*E*)-crotonaldehyde (8.94 vs. 1.62 eV). This indicates that the former is a much more powerful electrophile (defined within the *ω* scale), increasing the polarity of the DA reaction (as measured by the amount of charge transferred from the diene to the dienophile along the TS).[13] On the other hand, the computed differences between C*α* and C*β* P^+_k (Parr function on atom *k*) are higher for (***E***)**-Im-5Ba** than that for (*E*)-crotonaldehyde (ΔP^+_k = 0.76 vs. 0.47), suggesting that more asynchronous transition structures should be expected for the iminium-derived dienophile.[14]

Within the distortion/interaction model, the activation energy ($\Delta E^{\ddagger}$) is decomposed as the sum of the distortion energy ($\Delta E_d^{\ddagger}$, energy required to distort the reactants from their initial geometries to their transition state geometries) and the interaction energy $\Delta E_i^{\ddagger}$ (binding energy between the deformed reactants in the transition state, normally a negative value).[15] It has been recently found that polar and asynchronous DA reactions afford highly interacted and low distorted TS, leading to low energy barriers.[14] In this case, the $\Delta E^{\ddagger}$ computed for the reaction between (***E***)**-Im-5Ba** and **7** are only 3.0 kcal/mol (8.8 kcal/mol in solution), much lower than the 20.9 kcal/mol (20.9 kcal/mol in solution) calculated for the uncatalyzed cycloaddition of **7** and **9**. As expected from the conceptual DFT analysis, the charge transfer found for **TS-**(***E***)**-Im-5Ba+7** is 0.41e, ∼2.9 times higher than that computed for **TS-9** + **7** (0.14e). As a consequence, $\Delta E_i^{\ddagger}$ is much lower for the former (−21.3 kcal/mol vs. −8.6 kcal/mol). Moreover, the asynchronicity, Δ*d* (defined as the difference in the two bond forming distances at the TS) is higher for **TS-**(***E***)**-Im-5Ba+7** (0.99 Å vs. 0.34 Å), leading to lower $\Delta E_d^{\ddagger}$ (24.2 kcal/mol vs 29.5 kcal/mol).[17]

Such difference in energy barriers is fully consistent with the rate increase experimentally found for the organocatalyzed cycloaddition. In addition, these barriers indicated that >99.9% of the reagents should react via the catalyzed path (based on the activation barriers difference and assuming that the rate of formation and hydrolysis of the iminium are much faster than the thermal DA path), and the enantioselectivity of the process can be predicted, at least in principle, from the analysis of the competing iminium-derived transition structures.

In this context, we planned to experimentally demonstrate the formation of an iminium ion intermediate. The ^{1}H NMR spectra of **5Ba** in CD_3OD were recorded prior to and after the addition of 1 equiv of TFA and 5 equiv of (*E*)-cinnamaldehyde, in that order.[17] Apart from the ^{1}H NMR shifts of **6** and

DOI: 10.1021/acs.joc.5b01214
J. Org. Chem. 2015, 80, 7626−7634

protonated **5Ba** (**5Ba-H**), we were able to detect signals consistent with the formation of an iminium ion in a 1:2.7 ratio (relative to **5Ba-H**). The ^{1}H NMR of **5Ba-H** showed chemical shifts of H-7 and the methyl group at C-8 at δ_H 5.36 and 1.71 ppm, respectively (Figure 3). In comparison, those signals were

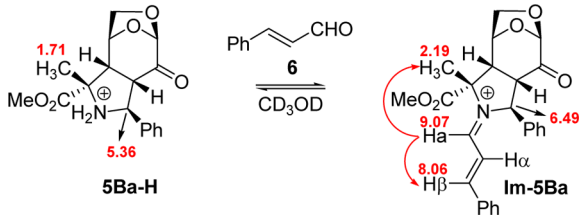

Figure 3. Key ^{1}H NMR signals of **5Ba-H** and **Im-5Ba**, and NOE correlations (red arrows).

shifted downfield to δ_H 6.49 ($\Delta\delta_H$ 1.13 ppm) and 2.19 ppm ($\Delta\delta_H$ 0.48 ppm), respectively, in the intermediate. This, along with the observation of key resonances at δ_H 9.07 ppm (dd, J = 10.9 Hz, J = 1.8 Hz) and δ_H 8.06 ppm (d, J = 15.2 Hz), were fully consistent with the formation of the proposed iminium. The last two signals were assigned to Ha and Hβ of **Im-5Ba** (Figure 3) based on the evident similarity to those reported for the iminium ion obtained from the condensation of MacMillan imidazolidinone and **6** (δ_H 9.05 ppm and δ_H 8.15 ppm, respectively).[16] Further evidence for our assignment came from NOE experiments: irradiation at Ha (δ_H 9.07 ppm) resulted in an enhancement of the signals of Hβ and the methyl group at C-8 (Figure 3).[17] This finding allowed us to establish that the preferred geometry of **Im-5Ba** is (*E*), in line with our computational results discussed above (Figure 2).

The sense of asymmetric induction experimentally found for **5Ba** is consistent with selective approach of cyclopentadiene from the less hindered (*Re*) face of (*E*)-**Im-5Ba**. In fact, all competing transition structures were next located at the B3LYP/6-31G* level of theory (Figure 4 shows the most stable conformers found for each mode of addition). In all cases, the TSs are highly asynchronous, with the C−C bond formation involving the C-β of the dienophile (the most electrophilic center) almost fully developed (1.99−2.05 Å), while the second C−C bond is only emerging (3.02−3.04 Å). The calculated relative activation energies reflect excellent agreement with the experimental findings. As expected, the TSs arising from the (*E*)-**Im-5Ba** are 1.9−3.7 kcal/mol more stable than those resulting from the (*Z*)-iminium geometries. Good facial discrimination (1.6 kcal/mol) was computed for the (*E*)-**Im-5Ba**+**7** TSs, mainly because repulsive steric interactions between cyclopentadiene and the phenyl ring were directed toward the β-face of the molecule. The Boltzmann distribution using all stable conformers found for each reaction channel predicts the *exo*-(2*R*)-product formation in 78% ee, close to the experimentally found value of 72% ee.[17]

The enantioselection could be fairly predicted by standard DFT methods, leading to the paramount opportunity to perform an in silico screening of new organocatalysts. However, considering the size of the present systems, the CPU time would be prohibitively long for rational design purposes, even at the often affordable B3LYP/6-31G* level of theory. To overcome this limitation, we considered the use of the hybrid ONIOM method.[18] In this approach, the small core region involving bond-forming and bond-breaking events are modeled using a high level of theory, while the rest of the system is

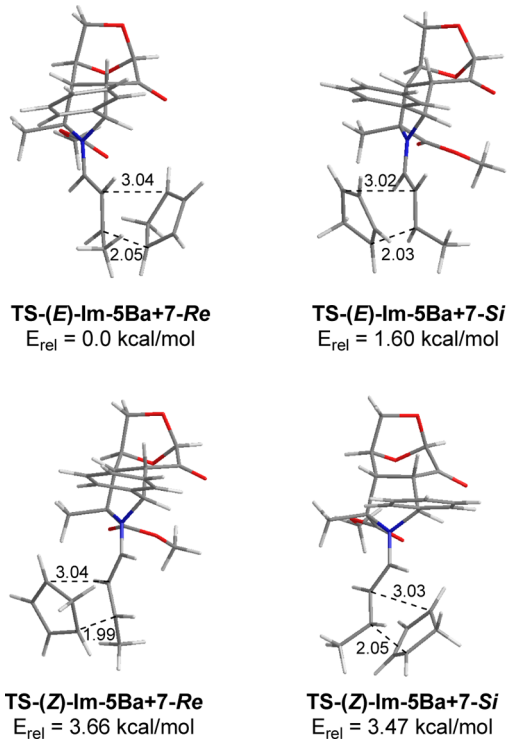

Figure 4. B3LYP/6-31G*-optimized geometries for the TSs (global minima) found for each mode of addition in the reaction between **Im-5Ba** and **7**. Selected distances are given in angstroms.

treated with a less accurate model. The energy of the *real* system at the *high level* can be estimated using an extrapolation scheme as $E_{(ONIOM,real)} = E_{(high,model)} + E_{(low,real)} - E_{(low,model)}$. The stereoselectivity of a wide variety of organic reactions could be fairly explained using this approach,[19] but to the best of our knowledge, there are no background on the use of ONIOM in iminium-based asymmetric Diels−Alder reactions. Intrigued by whether such a computational method could provide accurate prediction of the stereochemical outcome in the studied reactions, we selected a small data set composed of eight secondary amines that had been already tested as chiral organocatalysts in the DA reaction between (*E*)-cinnamaldehyde and cyclopentadiene (Figure 5).

Amines **10A**−**D** were taken from the seminal publication of MacMillan,[8a] while the remaining four were evaluated in the present work. The data set was chosen to provide structural

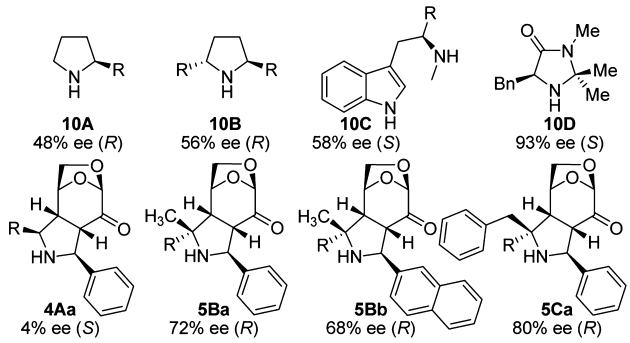

Figure 5. Set of eight secondary amines that were used as chiral organocatalysts in DA reactions between **6** and **7** (R = CO_2Me). The ee's correspond to the experimental selectivity toward the *exo* adduct.

DOI: 10.1021/acs.joc.5b01214
J. Org. Chem. 2015, 80, 7626−7634

diversity and a broad range of experimental ee's (ranging from 4 to 93% ee). To reduce the computational cost, we used (*E*)-crotonaldehyde (**9**) instead of (*E*)-cinnamaldehyde (**6**), and only the *exo* transition structures were taken into consideration.[20] Figure 6 illustrates the optimal partitioning scheme

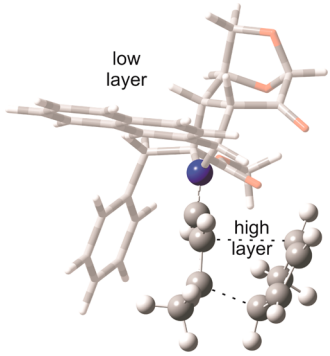

Figure 6. ONIOM(B3LYP/6-31G*:AM1) partition scheme. Grayed-out regions (low layer) were treated with AM1, and the full-colored regions (high layer) were treated with B3LYP/6-31G*.

that, after preliminary trials, afforded best results at a minimal computational cost. The reacting system (α,β-insaturated iminium and cyclopentadiene fragments) was optimized at the B3LYP/6-31G* level of theory, while the remainder of the system was treated using the semiempirical method AM1. Poor results were obtained using molecular mechanics in the lower layer (MMFF) as well as using the ONIOM(B3LYP/6-31G*:AM1) relative energies to compute the enantioselection of each catalyst. In contrast, B3LYP/6-31G* single-point energies with the polarizable continuum model (PCM) on the optimized ONIOM structures with methanol as solvent provided good agreement with the magnitude of the stereoselectivities.

Table 2 shows the enantioselectvity computed for each organocatalyzed reaction using a Boltzmann distribution of all

Table 2. Experimental and Calculated Enantioselectivity in the DA Reactions between 6 and 7 Catalyzed by the Chiral Amines Shown in Figure 5 at the PCM/B3LYP/6-31G*//ONIOM(B3LYP/6-31G*:AM1) Level of theory

entry	cat.	*exo* ee (%) exptl	*exo* ee (%) calcd
1	**10A**	48 (2*R*)	48 (2*R*)
2	**10B**	56 (2*R*)	52 (2*R*)
3	**10C**	58 (2*S*)	50 (2*S*)
4	**10D**	92 (2*S*)	92 (2*S*)
5	**4Aa**	4 (2*S*)	14 (2*R*)
6	**5Ba**	72 (2*R*)	80 (2*R*)
7	**5Bb**	68 (2*R*)	82 (2*R*)
8	**5Ca**	80 (2*R*)	96 (2*R*)

significantly populated conformers (up to 5.0 kcal/mol of the lowest energy TS).[17] The agreement between experimental and calculated data is noteworthy, both qualitatively (i.e., the sense of stereoinduction is correct) and quantitatively. It is also important to point out the impressive reduction in CPU time that was achieved with this method (more than 40 times faster than standard B3LYP/6-31G* treatment).

With this model in hand, we foresaw the in silico screening of catalysts with the **5B** core and different R_2 groups at C-7 as the structural element to modulate the catalyst's enantioselection. We then decided to evaluate the inductive capacity of 62 catalysts (Figure 7) that were selected to provide a wide array of molecular diversity and because of the commercial availability and affordable cost of the corresponding aldehyde precursor.[17]

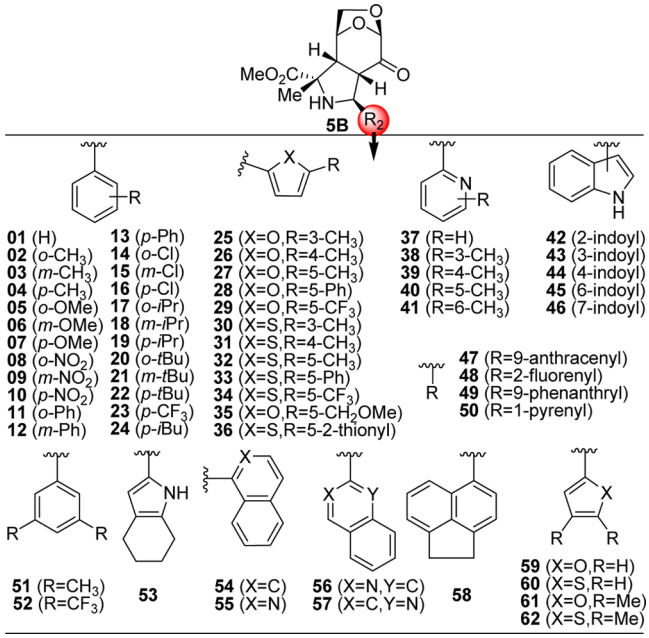

Figure 7. Sixty-two catalysts (**5B-01**−**5B-62**) chosen for in silico screening.

In an additional simplification, all transition structures arising from the (*Z*)-iminium ion were neglected, as they were found to be much higher in energy and not contributing significantly to the overall selectivity.[17] Once the calculations were done, the predicted $\Delta\Delta E^{\ddagger}$ values were translated into enantioselectivity values at 25 °C using Boltzmann averaging (Figure 8).[17]

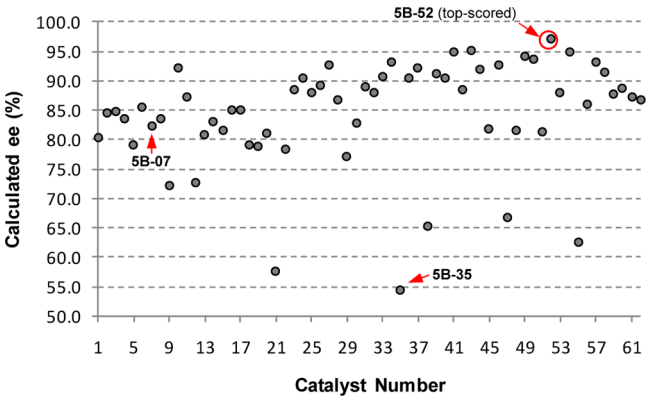

Figure 8. Calculated ee versus catalyst number.

The top-scored catalyst was compound **5B-52**, bearing a 3,5-bis(trifluoromethyl)phenyl substituent at the R_2 position. This result was promising as such a structural motif is present in many highly asymmetric inductors.[21] The selected compound was next synthesized following our previously reported general procedure (Scheme 2).[7] Iminoester **11B-52** was prepared in good yield from condensation of commercially available 3,5-

DOI: 10.1021/acs.joc.5b01214
J. Org. Chem. 2015, 80, 7626−7634

Scheme 2. Synthesis of the in Silico Top-Scored Screened Catalyst 5B-52 (R = CO_2Me)

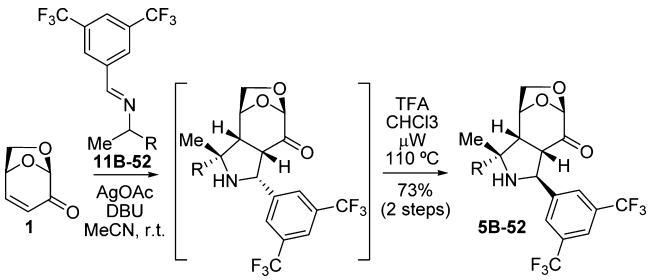

bis(trifluoromethyl)benzaldehyde and alanine methyl ester hydrochloride. Reaction of levoglucosenone (**1**) with **11B-52** in the presence of catalytic silver acetate and DBU yielded the expected *endo* isomer, which after a short column chromatography to eliminate silver salts and excess of iminoester was immediately heated in a 5:95 TFA/$CHCl_3$ solution at 110 °C for a period of 40 min using microwave irradiation. The desired compound **5B-52** was obtained in 73% overall yield, and its structure was inequivocally corroborated after extensive NMR experiments.[17]

With the new catalyst in hand, we were excited to find excellent results when using it in the DA reaction between **6** and **7** at the standard reaction conditions (96% yield, *exo*/*endo* 71:29, 90% ee and 92% ee for the *exo* and *endo* isomers, respectively, entry 1, Table 3). It is important to point out that such enantioselection could not be achieved with any of the 21 pyrrolidines experimentally evaluated before (Table 1), highlighting the relevance of the in silico screening. To further evaluate the ranking ability of our ONIOM-based computational method, we synthesize two additional catalysts: compounds **5B-07** and **5B-35** (highlighted in Figure 8) bearing a *p*-methoxyphenyl and 5-(methoxymethyl)-2-furyl substituent at the C-7 position. These compounds were taken as representative examples of medium- and low-scored catalysts, respectively, and were synthesized in 83% and 80% overall yield as described for **5B-52**.[17] Both pyrrolidines were tested in the standard DA reaction between **6** and **7** and afforded very good results in terms of yields (99%) and *exo* selectivity (81:19 and 75:25, respectively). Regarding the enantioselectivities, we were glad to find that the experimental values (72% ee and 56% ee, respectively) were in good accord with our predictions (82% ee and 54% ee, respectively), strengthening our confidence in the computational model.[17] Moreover, as discussed above, the catalysts **5C** (R_1 = Bn) afforded slightly higher selectivities than those with the **5B** (R_1 = Me) core, though with a significant decrease in the reactivity (Table 1). Therefore, we wondered whether the introduction of a 3,5-bis(trifluoromethyl)phenyl moiety at the C-7 position of **5C** would led to even better enantiomeric ratios than those obtained with **5B-52**. The performance of the resulting catalyst (**5C-52**, R_1 = Bn, R_2 = 3,5-$(CF_3)_2C_6H_3$) was evaluated in silico using our ONIOM approach. Interestingly, the prediction (90% ee) was lower than the computed values for **5B-52** (97% ee), suggesting that such structural modification would not be favorable in the former. To validate this result, compound **5C-52** was sinthesized in 70% overall yield and was evaluated in the DA reaction between **6** and **7** at the standard conditions. After 48 h, the desired adducts **8** were isolated in 66% yield, *exo*/*endo* 69:31, 76% ee and 86% ee for the *exo* and *endo* isomers, respectively.[17] Thus, in line with the computational results, the introduction of a 3,5-$(CF_3)_2C_6H_3$ group at the C-7 position of **5C** did not improve its catalytic activity.

The effect of the reaction conditions in the outcome of the DA reaction between **6** and **7** catalyzed by the in silico optimized **5B-52** was next evaluated in detail (Table 3). Several acids were investigated as cocatalysts (entries 1−6), and we found that the reaction proceeded poorly in the presence of the weaker acids $PhCO_2H$ and H_3PO_4. In contrast, strong acids ($HClO_4$, HCl, TFA, CSA) performed well in terms reactivity and selectivity, though slightly better enantioselectivities were obtained with the former. Screening of solvents (entries 1, 6−13) indicated that although THF was not suitable, a wide variety of aqueous solvents (MeOH, EtOH, CH_2Cl_2, MeCN, H_2O) afforded good results. Lower selectitivies were observed with acetonitrile (entry 9), while the highest levels of *exo*/*endo* ratio and ee's were obtained with MeOH/H_2O 9:1 (entry 1). Higher (entry 12) or lower (entry 13) water content in the

Table 3. Effect of the Reaction Conditions on the Diels−Alder Reaction between (*E*)-Cinnamaldehyde (6) and Cyclopentadiene (7) Catalyzed by 5B-52[a]

entry	**5B-52** (mol %)	Co-catalyst (mol %)	solvent	temp (°C)	time (h)	yield[b] (%)	*exo*/*endo*[c,d]	*exo* ee[d] (%)	*endo* ee[d] (%)
1	15	$HClO_4$ (15)	MeOH/H_2O 9:1	rt	12	96	71:29	90	92
2	15	TFA (15)	MeOH/H_2O 9:1	rt	12	99	70:30	84	94
3	15	HCl (15)	MeOH/H_2O 9:1	rt	12	99	70:30	84	92
4	15	CSA (15)	MeOH/H_2O 9:1	rt	12	92	70:30	84	92
5	15	$PhCO_2H$ (15)	MeOH/H_2O 9:1	rt	60	42	69:31	82	80
6	15	H_3PO_4 (15)	MeOH/H_2O 9:1	rt	12	50	70:30	84	90
7	15	$HClO_4$ (15)	EtOH/H_2O 9:1	rt	12	93	69:31	84	92
8	15	$HClO_4$ (15)	DCM/H_2O 9:1	rt	12	93	72:28	86	88
9	15	$HClO_4$ (15)	MeCN/H_2O 9:1	rt	12	97	64:36	76	90
10	15	$HClO_4$ (15)	THF/H_2O 9:1	rt	12	38	65:35	82	92
11	15	$HClO_4$ (15)	H_2O	rt	12	95	67:33	82	90
12	15	$HClO_4$ (15)	MeOH/H_2O 7:3	rt	12	99	71:29	84	90
13	15	$HClO_4$ (15)	MeOH/H_2O 99:1	rt	12	99	70:30	88	92
15	5	$HClO_4$ (5)	MeOH/H_2O 9:1	rt	12	88	69:31	84	92
16	15	$HClO_4$ (15)	MeOH/H_2O 9:1	0	12	82	68:32	92	97

[a]General reaction conditions: 5 equiv of cyclopentadiene. [b]Isolated yield after column chromatography. [c]Determined by ^1H NMR. [d]Determined by chiral GC.

DOI: 10.1021/acs.joc.5b01214
J. Org. Chem. 2015, 80, 7626−7634

methanolic solvent mixture gave slightly lower *exo* ee's. Though we have used 15 mol % of catalyst in the above reactions, loading can be reduced to 5 mol % with minor effects in the reaction outcome. Moreover, running the reactions at 0 °C allowed us to increase the enantioselection of the process (*exo* 92% ee, *endo* 97% ee), reaching the levels of selectivity found for leading organocatalysts.[8] Finally, as an additional important feature of our system, it is noteworthy that compound **5B-52** could be recovered quantitatively after workup and column chromatography and reused more than five times with no evident loss in its catalytic capacity. The ease of recovery represents a key aspect in modern organocatalysis, and much effort has been made in the immobilization of known organocatalysts in solid supports to facilitate the recycling process.[22]

CONCLUSIONS

An efficient organocatalyst for iminium ion based asymmetric DA reactions has been rationally designed combining experimental, NMR, and computational studies. The most influential structure−activity relationships were determined experimentally, while DFT calculations and NMR studies provided further mechanistic insight. This knowledge guided an in silico screening of 62 different catalysts using an ONIOM-(B3LYP/6-31G*:AM1) transition-state modeling, which showed good correlation between theory and experiment. The top-scored compound was easily synthesized from levoglucosenone, a biomass-derived chiral enone, and evaluated in the DA reaction between (*E*)-cinnamaldehyde and cyclopentadiene. In line with the computational finding, excellent results (up to 97% ee) were obtained. To the best of our knowledge, this type of methodology has no precedent in the development of efficient asymmetric organocatalysts. In addition, the novel catalyst is easily prepared from renewable sources and can be recovered and reused with no loss in its catalytic activity. Current studies on the use of this catalyst in other iminium-promoted transformations are currently being undertaken and will be published in due course.

COMPUTATIONAL DETAILS

All DFT calculations were carried out with the B3LYP[23] exchange-correlation functional coupled with the standard 6-31G* basis set using Gaussian 09.[24] All stationary points were characterized by frequency calculations, and all TSs were confirmed to have only one imaginary frequency corresponding to the formation of the expected bonds. The CT were computed with the natural bond order (NBO) method.[25] The global electrophilicity index, ω, was computed according to the following expression, $\omega = \mu^2/2\eta$ (eV), where μ is the electronic chemical potential and η the chemical hardness. Both quantities were estimated on the basis of the one-electron energies from the HOMO and LUMO, ε_H and ε_L, as $\mu \sim (\varepsilon_H + \varepsilon_L)/2$ and $\eta \sim (\varepsilon_L - \varepsilon_H)$.[26] The P^+_k (electrophilic Parr function of atom k), was computed using the Mulliken atomic spin density (ASD) by single-point UB3LYP/6-31G* calculations of the anion resulting from adding one electron to the optimized neutral B3LYP/6-31G* geometry.[27] The in silico screening was carried out as follows. Extensive conformational searches were performed to locate the most stable conformations of all competing transition structures. First, a large number of geometries were generated to explore the conformational space of the low region of the molecule with the MM+ force field[28] (as implemented in Hyperchem)[29] while keeping the high region frozen at the B3LYP/6-31G* geometry. All structures were then reoptimized using the ONIOM(B3LYP/6-31G*:AM1) level of theory using the partition scheme discussed above. Finally, B3LYP/6-31G* single-point energy calculations with the polarizable continuum model (PCM)[30] using methanol as solvent were performed on the resulting structures and were used to correct the gas-phase energies derived from the ONIOM calculations. The *exo* *R*/*S* ratios were computed using Boltzmann factors based on the relative energies in solution of all competing TSs.

EXPERIMENTAL SECTION

Microwave heating was performed in a CEM Discover System using septum-sealed 10 mL vials for high-pressure reaction conditions with stirring and IR-monitored temperature control. All reagents and solvents were used directly as purchased or purified according to standard procedures. Analytical thin-layer chromatography was carried out using commercial silica gel plates, and visualization was effected with short wavelength UV light (254 nm) and a *p*-anisaldehyde solution (2.5 mL of *p*-anisaldehyde + 2.5 mL of H_2SO_4 + 0.25 mL of AcOH + 95 mL of EtOH) with subsequent heating. Column chromatography was performed with silica gel 60 H, slurry packed, run under low pressure of nitrogen. NMR spectra were recorded at 300 MHz for ^{1}H and 75 MHz for ^{13}C with $CDCl_3$ as solvent and $(CH_3)_4Si$ (^{1}H) or $CDCl_3$ (^{13}C, 76.9 ppm) as internal standard. Chemical shifts are reported in delta (δ) units in parts per million (ppm), and splitting patterns are designated as s, singlet; d, doublet; t, triplet; q, quartet; m, multiplet; br, broad. Coupling constants are recorded in hertz (Hz). Isomeric ratios were determined by ^{1}H NMR analysis. The structure of the products was determined by a combination of spectroscopic methods such as IR, 1D and 2D NMR (including NOE, DEPT, COSY, HSQC and HMBC experiments), and HRMS. Infrared spectra were recorded using sodium chloride plate pellets. Absorbance frequencies are recorded in reciprocal centimeters (cm^{-1}). High-resolution mass spectra (HRMS) were obtained on a TOF-Q LC-MS spectrometer. Optical rotations were determined using a digital polarimeter in 100 mm cells and the sodium D line (589 nm) at room temperature in the solvent and concentration indicated. The melting points are uncorrected. Levoglucosenone (**1**) was prepared from microwave-assisted pyrolysis of acid-pretreated microcrystalline cellulose.[6d] The 21 pyrrolidines shown in Table 1 were synthesized following the procedure developed by our group.[7] The α-imino esters **11B-07**, **11B-35**, **11B-52**, and **11C-52** were prepared by condensation of the alanine or phenylalanine methyl ester hydrochloride and the corresponding aldehyde according to known procedures.[31]

General Procedure for the Synthesis of the Levoglucosenone-Derived Organocatalysts. To a solution of **1** (126 mg, 1 mmol) and the corresponding α-iminoester **11** (1.5 mmol) in dry MeCN (10 mL) were successively added AgOAc (50 mg, 0.3 mmol) and DBU (45 μL, 0.3 mmol). The mixture was stirred for 1 h at room temperature under argon atmosphere and in the absence of light (flask covered in aluminum foil). After filtration through Celite, the filtrate was concentrated to dryness under reduced pressure. The residue was filtered through a shot path of silica gel, concentrated to dryness, and dissolved in a 95:5 $CHCl_3$/TFA solution (2 mL). The resulting solution was stirred at 110 °C in the microwave reactor until complete conversion of the starting material (tipically 40 min). The solvent was removed under reduced pressure, and the crude was purified by column chromatography with elution with mixtures of hexanes and ethyl acetate to afford pure compound **5B-07** (83%), **5B-35** (80%), **5B-52** (73%), or **5C-52** (70%).

*Adduct **5B-07**:* white solid; mp = 152−153 °C (Hex/CH_2Cl_2); $[\alpha]_D$ −96.9 (*c* 1.27, $CHCl_3$); IR (KBr) ν_{max} 3358, 2953, 2849, 1738, 1732, 1614, 1510, 1246, 1165, 1111, 1036, 982 cm^{-1}; ^{1}H NMR ($CDCl_3$) δ 7.41 (d, *J* = 8.6 Hz, 2H, arom), 6.86 (d, *J* = 8.6 Hz, 2H, arom), 5.11−5.04 (m, 2H, H-1 and H-7), 4.90 (d, *J* = 4.8 Hz, 1H, H-5), 3.95 (dd, *J* = 7.3 Hz, *J* = 4.8 Hz, 1H, H-6*exo*), 3.89 (dd, *J* = 7.3 Hz, *J* = 0.7 Hz, 1H, H-6*endo*), 3.79 (s, 3H, H-12), 3.68 (s, 3H, H-10), 2.96 (dd, *J* = 4.5 Hz, *J* = 10.3 Hz, 1H, H-3), 2.52 (d, *J* = 10.3 Hz, 1H, H-4), 2.21 (s, 1H, NH), 1.58 (s, 3H, H-11); ^{13}C NMR ($CDCl_3$) δ 198.4 (C, C-2), 176.0 (C, C-9), 158.5 (C, arom), 137.2 (C, arom), 127.4 (CH,2C arom), 113.7 (CH, 2C arom), 100.7 (CH, C-1), 71.9 (CH, C-5), 68.8 (CH_2, C-6), 66.4 (C, C-8), 59.9 (CH, C-7), 55.2 (CH_3, C-12), 54.9 (CH, C-4), 53.2 (CH, C-3), 52.2 (CH3, C-10), 25.0 (CH3,

DOI: 10.1021/acs.joc.5b01214
J. Org. Chem. 2015, 80, 7626−7634

C-11); HRMS-ESI calcd for $C_{18}H_{21}NNaO_6$ $[M + Na]^+$ 370.12666, found 370.12644.

Adduct **5B-35**: yellowish oil; $[\alpha]_D$ −10.9 (*c* 1,00, $CHCl_3$); IR (film) ν_{max} 3345, 2951, 2922, 2824, 1738, 1732, 1231, 1113, 980, 881, 797 cm^{-1}; ^1H NMR ($CDCl_3$) δ 6.24 (s, 2H, arom), 5.14−5.07 (m, 2H, H-1 and H-7), 4.90 (d, *J* = 3.6 Hz, 1H, H-5), 4.38 (d, *J* = 12.7 Hz, 1H, H-12a), 4.32 (d, *J* = 12.7 Hz, 1H, H-12b), 4.05−3.94 (m, 2H, H-6), 3.68 (s, 3H, H-10), 3.41−3.30 (m, 4H, H-13 and H-3), 2.62 (d, *J* = 10.0 Hz, 1H, H-4), 2.19 (s, 1H, NH), 1.56 (s, 3H, H-11); ^{13}C NMR ($CDCl_3$) δ 197.6 (C, C-2), 175.3 (C, C-9), 156.1 (C, arom), 151.1 (C, arom), 110.2 (CH, arom), 107.2 (CH, arom), 100.7 (CH, C-1), 72.0 (CH, C-5), 68.8 (CH_2, C-6), 66.6 (C, C-8), 66.3 (CH_2, C-12), 57.7 (CH_3, C-13), 55.8 (CH, C-4), 55.2 (CH, C-7), 52.3 (CH3, C-10), 50.0 (CH, C-3), 24.9 (CH_3, C-11); HRMS-ESI calcd for $C_{17}H_{21}NNaO_7$ $[M + Na]^+$ 374.12089, found 374.12102.

Adduct **5B-52**: yellowish oil; $[\alpha]_D$ −60.4 (*c* 0.73, $CHCl_3$); IR (film) ν_{max} 3346, 2976, 2909, 1738, 1732, 1435, 1381, 1171, 1126, 984, 683 cm^{-1}; ^1H NMR ($CDCl_3$) δ 8.02 (s, 2H, arom), 7.75 (s, 1H, arom), 5.27 (d, *J* = 4.7 Hz, 1H, H-7), 5.15 (s, 1H, H-1), 4.93 (d, *J* = 4.6 Hz, 1H, H-5), 3.98 (dd, *J* = 7.3 Hz, *J* = 4.8 Hz, 1H, H-6*exo*), 3.92 (d, *J* = 7.3 Hz, 1H, H-6*endo*), 3.71 (s, 3H, H-10), 2.93 (dd, *J* = 10.2 Hz, *J* = 4.7 Hz, 1H, H-3), 2.53 (d, *J* = 10.2 Hz, 1H, H-4), 1.63 (s, 3H, H-11); ^{13}C NMR ($CDCl_3$) δ 197.6 (C, C-2), 175.9 (C, C-9), 147.9 (C, arom), 131.5 (2C, q, *J* = 34.4 Hz, arom), 126.7 (CH, 2C, arom), 123.3 (2C, q, *J* = 270.9 Hz, CF_3), 120.8 (CH, arom), 100.5 (CH, C-1), 71.8 (CH, C-5), 68.8 (CH_2, C-6), 66.5 (C, C-8), 59.2 (CH, C-7), 54.3 (CH, C-4), 52.8 (CH, C-3), 52.4 (CH_3, C-10), 24.9 (CH_3, C-11); HRMS-ESI calcd for $C_{19}H_{17}F_6NNaO_5$ $[M + Na]^+$ 476.08910, found 476.09031.

Adduct **5C-52**: yellowish oil; $[\alpha]_D$ −99.7 (*c* 1,00, $CHCl_3$); IR (film) ν_{max} 3350, 3032, 2956, 2906, 1732, 1738, 1381, 1278, 1132, 983, 881, 758, 704, 682 cm^{-1}; ^1H NMR ($CDCl_3$) δ 7.95 (s, 2H, arom), 7.73 (s, 1H, arom), 7.34−7.24 (m, 5H, arom), 5.17−5.15 (m, 2H, H-1 and H-7), 5.10 (d, *J* = 4.8 Hz, 1H, H-5), 4.01 (dd, *J* = 7.5 Hz, *J* = 5.0 Hz, 1H, H-6exo), 3.92 (d, *J* = 7.6 Hz, 1H, H-6endo), 3.73 (s, 3H, H-10), 3.52 (d, *J* = 13.2 Hz, 1H, H-11a), 3.02 (d, *J* = 13.3 Hz, 1H, H-11b), 2.87 (dd, *J* = 10.4 Hz, *J* = 4.9 Hz, 1H, H-3), 2.64 (d, *J* = 10.4 Hz, 1H, H-4); ^{13}C NMR ($CDCl_3$) δ 197.7 (C, C-2), 174.9 (C, C-9), 148.1 (C, arom), 135.8 (C, arom), 131.6 (2C, q, *J* = 33.5 Hz, arom), 130.5 (CH, 2C, arom), 128.4 (CH, 2C, arom), 127.3 (CH, arom), 126.9 (CH, arom), 123.4 (2C, q, *J* = 270.0 Hz, CF_3), 120.9 (CH, arom), 100.6 (CH, C-1), 72.1 (CH, C-5), 70.5 (C, C-8), 69.0 (CH_2, C-6), 59.1 (CH, C-7), 52.6 (CH, C-3), 52.5 (CH_3, C-10), 52.3 (CH, C-4), 43.4 (CH_2, C-11); HRMS-ESI calcd for $C_{25}H_{21}F_6NNaO_5$ $[M + Na]^+$ 552.12161, found 552.12078.

Typical Procedure for Organocatalyzed Diels−Alder Reaction. To a solution of amine **5B-52** (0.09 mmol) in MeOH/H_2O 9:1 (2 mL) were added $HClO_4$ (0.09 mmol) and (*E*)-cinnamaldehyde (76 μL, 0.6 mmol) in that order. The solution was stirred at room temperature for 10 min, and cyclopentadiene (0.25 mL, 3 mmol) was next added. Upon consumption of the aldehyde (12 h), the solvent was removed under reduced pressure. The crude was dissolved in $CHCl_3$−H_2O−TFA 2:1:1 (2 mL) and stirred at room temperature for 2 h. Neutralization with satd aq $NaHCO_3$ and extraction with CH_2Cl_2 followed by column chromatography afforded compound **8**. Product ratios were determined by GC analysis: Supelco BetaDEX 325 (30 m × 0.25 mm), 60 °C, 2 °C/min gradient, 1 mL/min, *exo R* isomer t_R = 62.2 min, *exo S* isomer t_R = 62.7 min, *endo R* isomer t_R = 63.1 min, *endo S* isomer t_R = 63.5 min. NMR data of **8** were consistent with the previously reported values.[8a,b]

■ ASSOCIATED CONTENT

Supporting Information

Copies of ^1H and ^{13}CNMR spectra of new products and computational data associated with this paper. The Supporting Information is available free of charge on the ACS Publications website at DOI: 10.1021/acs.joc.5b01214.

■ AUTHOR INFORMATION

Corresponding Author

*E-mail: sarotti@iquir-conicet.gov.ar.

Notes

The authors declare no competing financial interest.

■ ACKNOWLEDGMENTS

This research was supported by CONICET, UNR, and ANPCyT (Argentina). G.G.G. thanks CONICET for the award of a fellowship.

■ REFERENCES

(1) (a) *Enantioselective Organocatalysis*; Dalko, P. I., Ed.; Wiley−VCH: Weinheim, 2007. (b) Pellissier, H. *Recent Developments in Asymmetric Organocatalysis*; The Royal Society of Chemistry: Cambridge, UK, 2010. (c) Grondal, C.; Jeanty, M.; Enders, D. *Nat. Chem.* **2010**, *2*, 167. (d) MacMillan, D. W. C. *Nature* **2008**, *455*, 304. (e) Erkkilä, A.; Majander, I.; Pihko, P. M. *Chem. Rev.* **2007**, *107*, 5416. (f) Mukherjee, S.; Yang, J. W.; Hoffmann, S.; List, B. *Chem. Rev.* **2007**, *107*, 5471. (g) Dalko, P. I.; Moisan, L. *Angew. Chem., Int. Ed.* **2004**, *43*, 5138. (h) Milo, A.; Neel, A. J.; Toste, F. D.; Sigman, M. S. *Science* **2015**, *347*, 737.

(2) (a) Jover, J.; Fey, N. *Chem. - Asian J.* **2014**, *9*, 1714. (b) Corbeil, C. R.; Moitessier, N. *J. Mol. Catal. A: Chem.* **2010**, *324*, 146. (c) Brown, J. M.; Deeth, R. J. *Angew. Chem., Int. Ed.* **2009**, *48*, 4476. (d) Houk, K. N.; Cheong, P. H. Y. *Nature* **2008**, *455*, 309.

(3) (a) Cheong, P. H-Y.; Legault, C. Y.; Um, J. M.; Çelebi-Ölçüm, N.; Houk, K. N. *Chem. Rev.* **2011**, *111*, 5042. For recent references, see: (b) Lam, Y.-H.; Houk, K. N. *J. Am. Chem. Soc.* **2015**, *137*, 2116. (c) Overvoorde, L. M.; Grayson, M. N.; Luo, Y.; Goodman, J. M. *J. Org. Chem.* **2015**, *80*, 2634. (d) Lam, Y.-H.; Houk, K. N. *J. Am. Chem. Soc.* **2014**, *136*, 9556. (e) Lee, R.; Zhong, F.; Zheng, B.; Meng, Y.; Lu, Y.; Huang, K.-W. *Org. Biomol. Chem.* **2013**, *11*, 4818. (f) Grayson, M. N.; Goodman, J. M. *J. Am. Chem. Soc.* **2013**, *135*, 6142.

(4) (a) Yang, H.; Wong, M. W. *J. Org. Chem.* **2011**, *76*, 7399. (b) Shinisha, C. B.; Sunoj, R. B. *Org. Lett.* **2009**, *11*, 3242. (c) Shinisha, C. B.; Sunoj, R. B. *Org. Biomol. Chem.* **2007**, *5*, 1287.

(5) (a) Odagi, M.; Furukori, K.; Yamamoto, Y.; Sato, M.; Iida, K.; Yamanaka, M.; Nagasawa, K. *J. Am. Chem. Soc.* **2015**, *137*, 1909. (b) Fleming, E. M.; Quigley, C.; Rozas, I.; Connon, S. J. *J. Org. Chem.* **2008**, *73*, 948. (c) Mitsumori, S.; Zhang, H.; Cheong, P. H-Y.; Houk, K. N.; Tanaka, F.; Barbas, C. F., III. *J. Am. Chem. Soc.* **2006**, *128*, 1040.

(6) (a) Witczak, Z. J., Ed. *Levoglucosenone and Levoglucosans: Chemistry and Applications*; ATL Press: Mount Prospect, 1994. (b) Corne, V.; Botta, M. C.; Giordano, E. D. V.; Giri, G. F.; Llompart, D. F.; Biava, H. D.; Sarotti, A. M.; Mangione, M. I.; Mata, E. G.; Suárez, A. G.; Spanevello, R. A. *Pure Appl. Chem.* **2013**, *85*, 1683. (c) Sarotti, A. M.; Zanardi, M. M.; Spanevello, R. A.; Suárez, A. G. *Curr. Org. Synth.* **2012**, *9*, 439. (d) Sarotti, A. M.; Spanevello, R. A.; Suárez, A. G. *Green Chem.* **2007**, *9*, 1137.

(7) Sarotti, A. M.; Spanevello, R. A.; Suárez, A. G.; Echeverría, G. A.; Piro, O. E. *Org. Lett.* **2012**, *14*, 2556.

(8) (a) Ahrendt, K. A.; Borths, C. J.; MacMillan, D. W. C. *J. Am. Chem. Soc.* **2000**, *122*, 4243. (b) Kano, T.; Tanaka, Y.; Maruoka, K. *Org. Lett.* **2006**, *8*, 2687. (c) Gotoh, H.; Hayashi, Y. *Org. Lett.* **2007**, *9*, 2859. (d) Bonini, B. F.; Capitò, E.; Comes-Franchini, M.; Fochi, M.; Ricci, A.; Zwanenburg, B. *Tetrahedron: Asymmetry* **2006**, *17*, 3135. (e) Hayashi, Y.; Samanta, S.; Gotoh, H.; Ishikawa, H. *Angew. Chem., Int. Ed.* **2008**, *47*, 6634. (f) He, H.; Pei, B.-J.; Chou, H.-H.; Tian, T.; Chan, W.-H.; Lee, A. W. M. *Org. Lett.* **2008**, *10*, 2421.

(9) Lemay, M.; Ogilvie, W. W. *J. Org. Chem.* **2006**, *71*, 4663.

(10) To reduce the computational cost, we used crotonaldehyde instead cinnamaldehyde.

(11) Geerlings, P.; De Proft, F.; Langenaeker, W. *Chem. Rev.* **2003**, *103*, 1793.

(12) Parr, R. G.; von Szentpaly, L.; Liu, S. *J. Am. Chem. Soc.* **1999**, *121*, 1922.

DOI: 10.1021/acs.joc.5b01214
J. Org. Chem. 2015, 80, 7626−7634

(13) Domingo, L. R.; Aurell, M. J.; Perez, P.; Contreras, R. *Tetrahedron* **2002**, *58*, 4417.
(14) Sarotti, A. M. *Org. Biomol. Chem.* **2014**, *12*, 187.
(15) van Zeist, W.-J.; Bickelhaupt, F. M. *Org. Biomol. Chem.* **2010**, *8*, 3118.
(16) Brazier, J. B.; Evans, G.; Gibbs, T. J. K.; Coles, S. J.; Hursthouse, M. B.; Platts, J. A.; Tomkinson, N. C. O. *Org. Lett.* **2009**, *11*, 133.
(17) For further details on this issue, see the Supporting Information.
(18) (a) Dapprich, S.; Komaromi, I.; Byun, K. S.; Morokuma, K.; Frisch, M. J. *J. Mol. Struct.: THEOCHEM* **1999**, *461*, 1. (b) Bersuker, I. B. *Comput. Chem.* **2001**, *6*, 69.
(19) (a) Grayson, M. N.; Pellegrinet, S. C.; Goodman, J. M. *J. Am. Chem. Soc.* **2012**, *134*, 2716. (b) Shinisha, C. B.; Sunoj, R. B. *Org. Biomol. Chem.* **2008**, *6*, 3921. (c) Zhang, X.; Du, H.; Wang, Z.; Wu, Y. D.; Ding, K. *J. Org. Chem.* **2006**, *71*, 2862. (d) Ananikov, V. P.; Szilagyi, R.; Morokuma, K.; Musaev, D. G. *Organometallics* **2005**, *24*, 1938. (e) Balcells, D.; Maseras, F.; Ujaque, G. *J. Am. Chem. Soc.* **2005**, *127*, 3624. (f) Dudding, T.; Houk, K. N. *Proc. Natl. Acad. Sci. U. S. A.* **2004**, *101*, 5770.
(20) (a) In general, little difference is found in the reactions between **6** or **9** with cyclopentadiene under the same reaction conditions (for example, see ref 8). (b) To reduce the computational cost of the present study, we chose to study only the *exo* channels of addition for two main reasons: (i) in our system, the *exo* adducts are the major isolated compounds; (ii) as a general trend (and as was experimentally found in this work), a good organocatalyst affords high levels of enantioselection for both *endo* and *exo* adducts (for other examples, see ref 8).
(21) (a) Parmar, D.; Sugiono, E.; Raja, S.; Rueping, M. *Chem. Rev.* **2014**, *114*, 9047. (b) Vakulya, B.; Varga, S.; Csámpai, A.; Soos, T. *Org. Lett.* **2005**, *7*, 1967. (c) Franzén, J.; Marigo, M.; Fielenbach, D.; Wabnitz, T. C.; Kjærsgaard, A.; Jørgensen, K. A. *J. Am. Chem. Soc.* **2005**, *127*, 18296. (d) Okino, T.; Hoashi, Y.; Takemoto, Y. *J. Am. Chem. Soc.* **2003**, *125*, 12672.
(22) (a) Puglisi, A.; Benaglia, M.; Annunziata, R.; Chiroli, V.; Porta, R.; Gervasini, A. *J. Org. Chem.* **2013**, *78*, 11326. (b) Hagiwara, H.; Kuroda, T.; Hoshi, T.; Suzuki, T. *Adv. Synth. Catal.* **2010**, *352*, 909. (c) Gruttadauria, M.; Giacalone, F.; Noto, R. *Chem. Soc. Rev.* **2008**, *37*, 1666. (d) Corma, A.; Garcia, H. *Adv. Synth. Catal.* **2006**, *348*, 1391. (e) Benaglia, M.; Puglisi, A.; Cozzi, F. *Chem. Rev.* **2003**, *103*, 3401.
(23) (a) Lee, C.; Yang, W.; Parr, R. G. *Phys. Rev. B: Condens. Matter Mater. Phys.* **1988**, *37*, 785. (b) Becke, A. D. *J. Chem. Phys.* **1993**, *98*, 1372. (c) Becke, A. D. *J. Chem. Phys.* **1993**, *98*, 5648.
(24) Frisch, M. J. et al. *Gaussian 09, Revision B.01*, Gaussian, Inc.: Wallingford, CT, 2009.
(25) NBO Version 3.1: Glendening, E. D.; Reed, A. E.; Carpenter, J. E.; Weinhold, F. For some original literature references, see:. (a) Reed, A. E.; Weinstock, R. B.; Weinhold, F. *J. Chem. Phys.* **1985**, *83*, 735. (b) Reed, A. E.; Curtiss, L. A.; Weinhold, F. *Chem. Rev.* **1988**, *88*, 899.
(26) (a) Parr, R. G.; Pearson, R. G. *J. Am. Chem. Soc.* **1983**, *105*, 7512. (b) Parr, R. G.; Yang, W. *Density Functional Theory of Atoms and Molecules*; Oxford University Press: New York, 1989.
(27) Domingo, L. R.; Pérez, P.; Sáez, J. A. *RSC Adv.* **2013**, *3*, 1486.
(28) Allinger, N. L. *J. Am. Chem. Soc.* **1977**, *99*, 8127−8134.
(29) Hyperchem Professional Release 7.52, Hypercube, Inc., 2005.
(30) For a review on continuum solvation models, see: Tomasi, J.; Mennucci, B.; Cammi, R. *Chem. Rev.* **2005**, *105*, 2999−3093.
(31) Cabrera, S.; Gómez Arrayás, R.; Martín-Matute, B.; Cossío, F.; Carretero, J. C. *Tetrahedron* **2007**, *63*, 6587.

DOI: 10.1021/acs.joc.5b01214
J. Org. Chem. 2015, 80, 7626−7634